

DESIGN AND OPTIMIZATION OF CHITOSAN-BASED NANOFIBROUS SCAFFOLD FOR THE DELIVERY OF NATURAL BIOACTIVE COMPOUNDS

Teodora Iurascu¹, Andreea-Teodora Iacob¹, Ana Maria Ipatov²,
Bianca-Ștefania Profire^{1*}, Lenuța Profire¹

1. Grigore T. Popa University of Medicine and Pharmacy Iasi, Romania

2. Alexandru Ioan Cuza University of Iasi, Romania

*Corresponding author. E-mail: bianca.profire@umfiasi.ro

DESIGN AND OPTIMIZATION OF CHITOSAN-BASED NANOFIBROUS SCAFFOLD FOR THE DELIVERY OF NATURAL BIOACTIVE COMPOUNDS (Abstract): The **aim** of this study was to obtain and optimize chitosan (CH)/poly(vinyl alcohol) (PVA)-based nanofibrous scaffold with controlled nanoscale characteristics, by identifying the key electrospinning parameters. The optimized scaffold was subsequently loaded with natural bioactive compounds (ACs). **Materials and methods:** To achieve an optimal polymer composition, different concentrations of each polymer and various CH/PVA ratios (v/v) were investigated until a formulation capable of generating uniform nanofibers (NFs) under experimentally optimized electrospinning conditions was obtained. Based on this optimized matrix six formulations were prepared: CH/PVA@ARG, CH/PVA@ARG-ALA, CH/PVA@ARG-RJ, CH/PVA@ALA, CH/PVA@CUR, and CH/PVA@CUR-ALA, by incorporating L-arginine (ARG), allantoin (ALA), royal jelly (RJ), and curcumin (CUR), known for their antioxidant, antiseptic, and wound-healing properties. Fiber morphology was initially assessed by optical microscopy, followed by detailed analysis using scanning electron microscopy (SEM) to confirm the fibrous architecture and determine the fiber diameter. **Results:** The optimization process yielded uniform, bead-free CH/PVA NFs at a 1:3 ratio and a total polymer concentration of 6.25%. The optimized matrix enabled the incorporating ACs at selected concentrations (10% ARG, 4% ALA, 3% CUR, 3% RJ). For synergistic combinations, concentration adjustments were required to preserve fiber morphology and avoid rheological instabilities associated with cumulative AC loading. **Conclusions:** CH/PVA@ACs NFs with uniform, bead-free fiber morphology suitable for wound healing applications, were prepared. **Keywords:** CHITOSAN, ACTIVE COMPOUNDS, OPTIMIZATION, ELECTRO-SPINNING.

INTRODUCTION

One of the main innovations in the development of advanced wound dressings is the application of nanotechnology. In this context, nanofibers (NFs) (nonwoven materials) synthesized by electrospinning represent one of the most promising and advantageous approaches. These NFs can mimic

the three-dimensional (3D) architecture of the extracellular matrix (ECM) and modulate cellular behavior, thereby promoting the cascade of processes involved in tissue regeneration (1). The term wound is a general concept, that describes several types of skin damage or injury. Wounds can be classified according to several criteria, such

Design and optimization of chitosan-based nanofibrous scaffold for the delivery of natural bioactive compounds

as: healing time, etiology, mechanism of injury, complexity, depth, degree of contamination, risk of post-operative infection and wound bed characteristics (2).

An effective wound dressing must satisfy three key requirements: it should be able to absorb exudate, alleviate pain, and protect the wound from secondary infections. In addition, the wound dressings to promote tissue repair and regeneration should have key properties, including antimicrobial activity, antioxidant potential, appropriate mechanical strength and biodegradability (3). Because the traditional gauze dressings have many disadvantages, including traumatic removal and a tendency to dehydrate the wound bed, new advance biomaterials have been developed. The modern dressings are designed to come into direct contact with the wound surface and to actively support tissue regeneration without inducing additional tissue damage. In clinical practice, NFs represent innovative dressings capable of providing controlled release of various active compounds (ACs) with important biological effects on wound healing, such as antioxidant, antibacterial, and immunomodulatory properties. In addition, NFs can maintain a moist, oxygenated, and sterile microenvironment that is essential for accelerated and effective wound healing. Furthermore, the development of composite biomaterials combining natural and synthetic polymers has led to improved biocompatibility, reduced toxicity, and enhanced wound-healing efficacy (4).

Chitosan (CH) is a polysaccharide composed of beta-(1-4)-linked 2-amino-2-deoxy-D-glucose (D-glucosamine) and N-acetyl-2-amino-2-deoxy-D-glucose (N-acetyl-D-glucosamine) units. It is obtained through alkaline deacetylation of chitin, which is extracted from the exoskeletons of

arthropods as well as from the cell walls of certain fungi (5). Owing to its favorable physicochemical and biological properties, including non-toxicity, biodegradability, biocompatibility, and intrinsic bioactivity, CH is an important natural polymer for biomedical applications (5). CH exhibits significant hemostatic effects due to interactions between its protonated amino groups (NH_3^+) and the negatively charged membranes of erythrocytes. In addition, CH exhibits analgesic properties by reducing bradykinin levels at the wound site, as well as anti-inflammatory effects, which is attributed to interactions between NH_3^+ groups and wound components, leading to attenuation of the inflammatory response (6). Furthermore, CH possesses antibacterial properties by forming a polymeric film around bacterial cells that inhibits cellular exchanges and nutrient transport (7-11).

Poli(vinyl alcohol) (PVA) is obtained through the free-radical polymerization of vinyl acetate, resulting in polyvinyl acetate (PVAc), followed by partial or complete hydrolysis of the acetate groups along the polymer backbone. During this process, acetate groups are replaced by hydroxyl (-OH) groups, and the degree of hydrolysis strongly influences the solubility, crystalline and physicochemical properties of the resulting PVA (12, 13). Due to its biocompatibility and low toxicity (14), PVA is frequently blended with natural polymers such as CH during electrospinning to produce NFs for tissue engineering applications (15).

L-Arginine (ARG) is an essential α -amino acid component of the urea cycle, a precursor to many biochemical pathways involved in cell physiology. ARG plays a key role in wound healing through two main mechanisms: (i) transformation of

ARG under the influence of arginase, with the obtaining of ornithine, precursor of L-proline, an important amino acid in the process of collagen synthesis; (ii) oxidative deamination of ARG, until obtaining nitric oxide (NO), a bioactive molecule involved in the processes of reepithelialization, cell proliferation, collagen synthesis and angiogenesis (16).

Allantoin (ALA), chemically known as 5-ureidohydantoin, is a natural compound that is widely regarded as safe for topical administration and exhibits low toxicity (17). ALA can be synthesized from urea and is also found biologically as an intermediate in the metabolism of certain plants and microorganisms, as well as a final product of purine catabolism in mammals. In mammals, it is formed via non-enzymatic degradation of uric acid in the absence of uricase, under the influence of reactive oxygen species (ROS) (18,19). ALA exhibits multiple biological effects, including antioxidant properties (20), anti-inflammatory activity, manifested by the reduction of pro-inflammatory cytokines, such as interleukin-1 (IL-1), interleukin-6 (IL-6), and tumor necrosis factor-alpha (TNF- α) (21), as well as keratolytic, moisturizing, and immunomodulatory properties (22).

Curcumin (CUR), is a polyphenolic complex derived from turmeric (*Curcuma longa L.*) that exhibits a broad spectrum of biological activities (3). Curcumin I is the main component, accounting for 60-70% of the total curcuminoid content, followed by demethoxycurcumin (curcumin II, 20-27%), and bisdemethoxycurcumin (curcumin III, 10-15%) (23). The scientific data indicate that curcumin I is largely responsible for the biological activity of the curcuminoid complex (3). It is widely recog-

nized for its antioxidant, antimicrobial, anti-inflammatory and antidiabetic properties (24, 25).

Royal jelly (RJ) is a highly valued natural product produced by honeybees (*Apis mellifera*), whose composition varies depending on bee species, botanical origin, and seasonal factors. It is primarily composed of water (50-60%), proteins (9-18%), carbohydrates (11-23%) and lipids (3-6%), and also contains vitamins (B complex, C, A, E), essential amino acids, minerals (Ca, Mg, Na, Cu, K, Mn, Fe, Zn), enzymes, hormones, polyphenols, nucleotides, and heterocyclic compounds (26-29). The beneficial effects of RJ in the treatment of skin disorders are largely attributed to its ability to reduce transepidermal water loss and to restore the lipid barrier (30), thereby maintaining an optimal degree of hydration at the wound site, which is essential for the healing process. In addition, RJ exhibits antifungal activity mainly due to royalisin (26), antimicrobial activity mediated by royalisin, jelleins (1-3), and the major RJ protein 4 (MRJP4) (22, 27-31), antibacterial effects associated with 10-hydroxy-2-decenoic acid (10-HDA), major RJ protein 2 (MRJP2), and MRJP4 (21, 22, 26), as well as antioxidant activity primarily attributed to its phenolic compounds and MRJP2 (22, 27).

The objective of this study was to design and optimize a CH/PVA-based nanofibrous matrix for the efficient encapsulation and delivery of the natural ACs such as CUR, ALA, ARG, and RJ.

MATERIALS AND METHODS

Reagents. Chitosan (CH) (medium molecular weight, 75-85% deacetylation grade), polyvinyl alcohol (PVA), 87-89% hydrolyzed, high molecular weight, aver-

Design and optimization of chitosan-based nanofibrous scaffold for the delivery of natural bioactive compounds

age M.W. 88.000-97.000 were purchased from Alfa Aesar; L-arginine (ARG), Allantoin ($\geq 98\%$ purity) (ALA), curcumin (CUR) analytical standard (M.W: 368.38) were purchase from Supelco; pure Royal jelly (RJ) was purchased from Melidava with 1.59 % (wt/wt) 10-Hydroxy-2-decenoic acid; glacial acetic acid ($\geq 99.7\%$) were purchased from Sigma Aldrich, distilled water (DW), tween 80.

Optimization of CH/PVA ratio for nanofibrous scaffold preparation

The optimization of CH and PVA blend ratio was systematically investigated to obtain nanofibrous scaffold with optimal characteristics, including reduced fiber diameter and bead-free structure. CH solutions (1%, 2%) were prepared by dissolving defined amounts of high molecular weight CH in glacial acetic acid, while PVA solutions (3%, 6%, 7%, 8%, 10%) were prepared by dissolving corresponding PVA amounts in deionized water under heating to ensure complete polymer dissolution. The two polymer solutions were subsequently combined in different volume ratios (CH: PVA - 1:1, 1:2, 1:3, 1:8, 2:6, 3:7) under continuous stirring for approximately 20 min, followed by equilibration at room temperature for 30 min to allow for air bubble removal. The resulting mixtures were stirred at room temperature until homogeneous solutions suitable for electrospinning were obtained.

Optimization of CH/PVA/ACs ratio for CH/PVA@ACs NFs preparation

After identifying the optimal CH:PVA ratio, ACs, namely CUR (1%, 2%, 3%, 4%), ALA (1%, 2%, 3%, 4%, 5%), ARG (1%, 3%, 5%, 10%, 15%), and RJ (1%, 2%, 3%, 4%), were incorporated at various concentrations. The resulting mixtures were stirred at room temperature until ho-

mogeneous solutions suitable for electrospinning were obtained.

Electrospinning process

The CH/PVA nanofibrous scaffold and CS/PVA@ACs NFs were prepared by electrospinning using a Nanospinner device (Inovenso) equipped with a high-voltage power supply, syringe pump, spinneret, and a grounded collector. The polymers solutions were loaded into a syringe serving as positive electrode, while the collector acted as the counter electrode. Electrospinning parameters, including the applied voltage, flow rate, and needle tip-to-collector distance were systematically optimized in conjunction with the polymer ratio to obtain uniform, bead-free NFs. The collected fibers were deposited on to aluminum foil and dried under room temperature prior to further characterization.

Characterization of the CH/PVA nanofibrous scaffold and CH/PVA@ACs NFs

CH/PVA nanofibrous scaffold and CH/PVA@ACs NFs, including single formulations (CH/PVA@ARG, CH/PVA@ALA, CH/PVA@CUR) as well as combined synergistic systems (CH/PVA@ARG-ALA, CH/PVA@ARG-RJ, CH/PVA@CUR-ALA), were first examined by macroscopic and low-magnification microscopic observation (40X) to verify the presence of continuous fibrous structures. Subsequently, fiber morphology and diameter were analyzed by scanning electron microscopy (SEM, In-spect S, 30 keV) (32). Prior to imaging, the samples were sputter-coated with a thin gold layer to minimize charge accumulation. Fiber diameter distributions were determined using *Phenom Fiber Metric* software, and the results are expressed as mean \pm standard deviation (SD) based on three independent measurements ($n = 3$).

RESULTS

In order to optimize the formulation for the fabrication of CH/PVA nanofibrous scaffold with uniform morphology, bead-free structure, high yield and reduced diameter, a series of processing and formulation parameters were systematically investigated through multiple experimental trials. Specifically, the effect of CH concentration (1%, 2% wt/v), PVA concentration (3%, 6%, 7%, 8%, 10%), CH: PVA polymer ratio (1:1, 1:2, 1:3, 2:6, 3:7, 1:8), applied voltage (13-17 kV), flow rate (0.1-0.3 mL/h), tip-to-collector distance (17-24 cm) and relative humidity (22-64%) were evaluated.

Based on the obtained results (tab. I),

the CH/PVA (1:3 v/v) formulation with a total polymer concentration of 6.25%, electrospun at an applied voltage of 17 kV, a flow rate of 0.25 mL/h, and a tip-to-collector distance of 20-24 cm, was identified as the optimal composition. This optimized formulation consistently yielded uniform, bead-free NFs, as confirmed by SEM analysis (fig. 1). The micrographs reveal the successful formation of an interconnected nanofibrous network with smooth fiber surfaces and homogeneous morphology, thereby validating the optimization strategy and establishing this composition as the base matrix for subsequent functionalization using natural ACs.

TABLE I.

Optimization of CH/PVA nanofibrous scaffold preparation

CH % (wt/v)	PVA % (wt/v)	CH: PVA (v/v)	Total polymer conc. (%)	Flow rate (mL/h)	Distance (cm)	Voltage (kV)	Microscopic morphology
1	3	1:1	0.6	0.1	17-22	13	polymeric fragments without a well-defined fibrous network
1	3	1:2	1.2	0.1	17-24	14	-
1	6	1:1	1.2	0.15	17-24	16	-
1	6	1:2	2.6	0.1-0.13	17-22	14	fibers with multiple beads interspersed among otherwise uniform fibers
1	6	3:7	4.3	0.13	17-22	13-15	-
1	7	1:2	3.0	0.13	20-24	14	uniform, bead-free fibers arranged in two layers, but with a reduced fiber production yield
1	8	2:6	5.0	0.3	20-24	17	-
2	8	1:8**	7.4	0.1-0.2	22-24	16	highly crowded fiber morphology
2	10	3:7**	7.6	0.1	18-20	12	-
1*	8*	1:3*	6.25*	0.25*	20-24*	17*	well-structured fibers with increased fiber density and ~ 100 nm diameter

*The parameters considered optimal used for obtaining the CH/PVA nanofibrous scaffold;

** One drop of tween 80 was added

Design and optimization of chitosan-based nanofibrous scaffold for the delivery of natural bioactive compounds

For the electrospinning of the CH/PVA@ACs polymeric solutions, the same ranges of process parameters used for CH/PVA polymeric solution were applied. In this case, the only variable was the con-

centration of ACs incorporated into the polymer matrix (tab. II). The resulting CH/PVA@ACs nanofibers (NFs) were subsequently characterized by macroscopic and microscopic analyses (fig. 2).

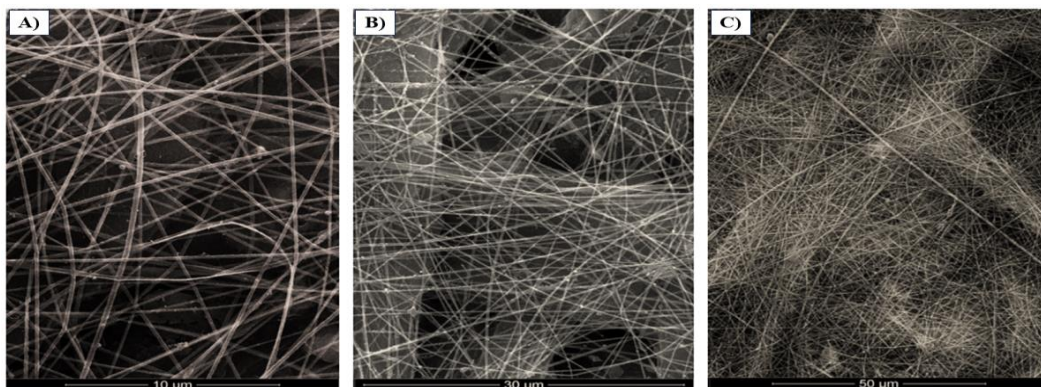


Fig. 1. Representative SEM images of electrospun CH/PVA nanofibrous scaffold at different scale bars: A) 10 μm ; B) 30 μm ; C) 50 μm

TABLE II.

Optimization of CH/PVA@ACs NFs preparation

CH/PVA@ACs	ACs conc. (wt/v)	Flow rate (mL/h)	Distance (cm)	Voltage (kV)
CH/PVA@ARG	ARG: 1%, 3%, 5%, 10%* , 15%	0.3	22	17
CH/PVA@ALA	ALA: 1%, 2%, 3%, 4%* , 5%	0.4	22	18
CH/PVA@CUR	CUR: 1%, 2%, 3%* , 4%	0.4	24	17
CH/PVA@ARG-ALA	ARG: 10% - ALA: 4% ARG: 10% - ALA: 3% ARG: 5% - ALA: 4% ARG: 5% - ALA: 3% ARG: 3% - ALA: 3%*	0.4	23	18
CH/PVA@ARG-RJ	ARG: 10% - RJ: 1% ARG: 10% - RJ: 2% ARG: 10% - RJ: 3%* ARG: 10% - RJ: 4%	0.3	16	15
CH/PVA@CUR-ALA	CUR: 4% - ALA: 4% CUR: 4% - ALA: 3% CUR: 3% - ALA: 3%*	0.3	26	16

*The ACs concentration (wt/v) considered optimal for obtaining the CH/PVA@ACs fibers

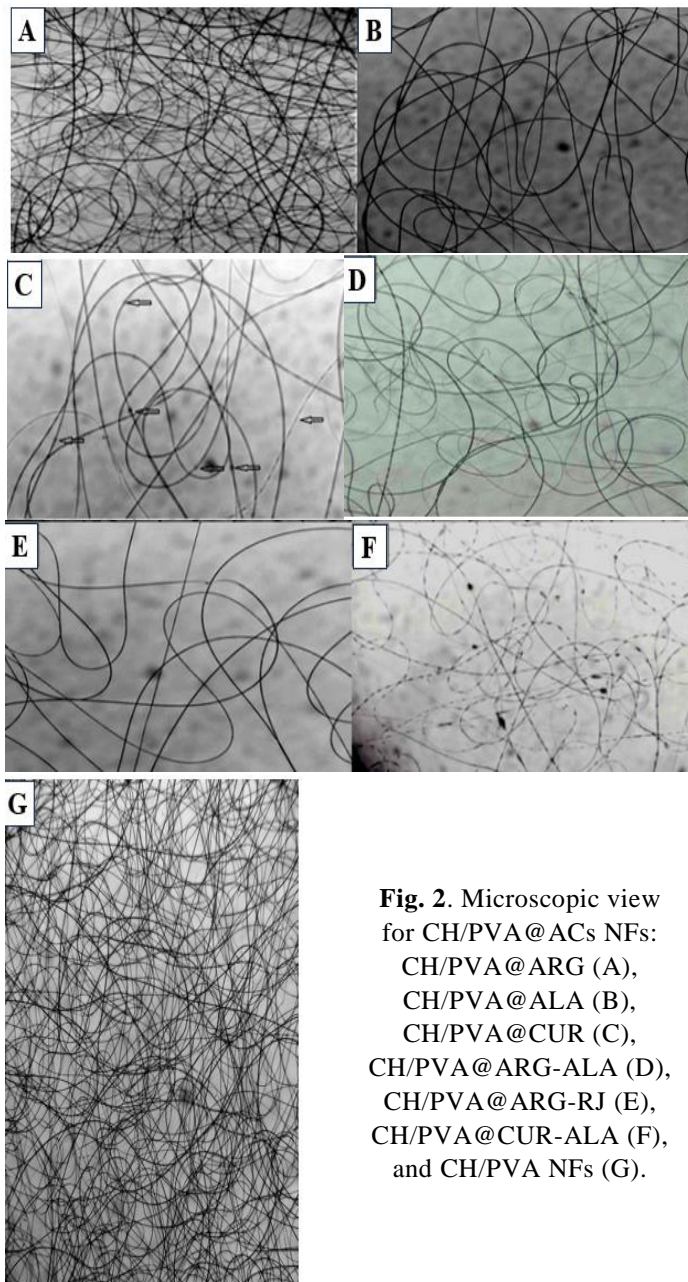


Fig. 2. Microscopic view for CH/PVA@ACs NFs: CH/PVA@ARG (A), CH/PVA@ALA (B), CH/PVA@CUR (C), CH/PVA@ARG-ALA (D), CH/PVA@ARG-RJ (E), CH/PVA@CUR-ALA (F), and CH/PVA NFs (G).

DISCUSSION

Analysis of the experimental data indicates that a minimum total polymer concentration of approximately 5% is required

to obtain uniform, small-diameter NFs, above which the nanofibrous production yield increases markedly. Below this threshold, bead-like structures and polymer

Design and optimization of chitosan-based nanofibrous scaffold for the delivery of natural bioactive compounds

fragments were predominantly observed, a behavior attributable to the low viscosity which is insufficient to stabilize the electro spun jet.

A progressive increase in the CH:PVA ratio in favor of PVA significantly improved fibers morphology. This effect can be explained by the formation of hydrogen bonds between PVA and the $-NH_2$, and $-OH$ groups of CH, which reduces surface tension and weakens the strong intramolecular interactions within CH chains. This trend is reflected by the morphological transition from polymer fragments (CH 1% /PVA 3%, 1:1) to continuous fibers (CH 1% /PVA 8%, 1:3). Moreover, the addition of a surfactant (tween 80) further facilitated nanofiber formation by lowering surface tension. The electrospinning process parameters exhibited a complex interdependence. For low-viscosity polymer solutions, increasing the applied voltage led to pronounced jet instability in the electric field. In addition, the optimal flow rate was found to be inversely related to the total polymer concentration, with values of 0.1 mL/h for 7.6%, total polymer and 0.2 mL/h for 7.4% total polymer.

All ACs were successfully incorporated into the polymer matrix at the desired concentrations, requiring only minor adjustments of the operating parameters, which highlights the versatility and robustness of the optimized CH/PVA base formulation. For synergistic combinations, AC concentrations were selected based on individually optimized values, while considering the maximum loading capacity of the CH/PVA matrix and the need to preserve stable electrospinning conditions. Simultaneous loading of ACs at their individual maximum concentration led to cumulative rheological disruptions, resulting in process instability.

The ARG concentration was therefore fixed at 10%, since preliminary experiments showed that increasing it to 15% caused excessive solution conductivity, which destabilized the electrospinning jet and promoted droplet formation instead of continuous fibers. In addition, bead formation and surface defects were observed, while enhanced electrostatic interactions between positively charged ARG and protonated CH induced visible solution inhomogeneities, necessitating extensive re-optimization of the process parameters. The combination of 10% ARG with 3% RJ was successfully achieved, with RJ being homogeneously incorporated into the polymer matrix without altering the optimized electrospinning parameters. Increasing the RJ concentration above 3% led to significant changes in the rheological properties, mainly due to a marked increase in viscosity associated with the molecular complexity and variability of RJ, which destabilized the jet and resulted in non-uniform fibers.

For ALA, the concentration was limited to 4%, as higher amounts revealed its limited solubility in the CH/PVA system, leading to presence of undissolved particles that blocked the electrospinning needle. Moreover, the associated viscosity changes disrupted the electrospinning parameters, resulting non-uniform fibers with morphological defects. Although increasing the temperature could potentially improve ALA solubility, this approach would have induced additional instability into the system. Consequently, the combination of 3% ARG with 3% ALA was selected in order to preserve the optimized electrospinning parameters.

The CUR concentration was limited to 3% due to its hydrophobic nature, which

led to suspension formation at higher loadings, even in the presence of DMSO. Furthermore, the crystalline character of CUR interfered with jet stability and resulted in non-uniform fibers morphologies. Attempts to maintain the same ALA concentration used in the individual formulation within the synergistic CUR-containing systems were unsuccessful, as no stable electrospinning system could be achieved and defective fibers were obtained

CONCLUSIONS

The optimization of CH/PVA nanofibrous scaffold and the establishment of optimal ACs concentrations, both in individual and synergistic combinations, through balancing of solution rheological

properties and electrospinning process stability, enabled the fabrication of nanofibers with the desired characteristics. This approach successfully addressed challenges related to limited solubility, viscosity variations, and cumulative rheological disruptions, while preserving the bioactivity of the incorporated natural compounds and ensuring reproducible fiber morphology.

CONFLICT OF INTEREST AND FUNDING

The authors declare that there is no conflict of interest. The research was supported by a grant of the Ministry of Education and Research CCCDI-UEFISCDI, project no. PN-IV-PCB-RO-MD-2024-0246, within PNCDI IV.

REFERENCES

1. Mei L, Fan R, Li X, *et al.* Nanofibers for improving the wound repair process: the combination of a grafted chitosan and an antioxidant agent. *Polym Chem* 2017; 8(10): 1664-1671.
2. Iacob AT, Drăgan M, Ionescu OM, *et al.* An Overview of Biopolymeric Electrospun Nanofibers Based on Polysaccharides for Wound Healing Management. *Pharmaceutics* 2020; 12(10): 983.
3. Alven S, Nqoro X, Aderibigbe BA. Polymer-Based Materials Loaded with Curcumin for Wound Healing Applications. *Polymers (Basel)* 2020; 12(10): 2286.
4. Bibire T. The development of alginate-based matrices loaded with Rifampicin for wound healing. *Med-Surg J - Rev Med Chir Soc Med Nat Iasi* 2024; 128(1): 167-176.
5. Qasim S, Zafar M, Najeeb S, *et al.* Electrospinning of Chitosan-Based Solutions for Tissue Engineering and Regenerative Medicine. *Int J Mol Sci* 2018; 19(2): 407.
6. Bibire T. Chitosan-gelatin micro/nanoparticles as a controlled delivery of Dexketoprofen trometamol for topical applications in wound care. *Med-Surg J - Rev Med Chir Soc Med Nat Iasi* 2024; 128(2): 411-421.
7. Abbas M, Hussain T, Arshad M, *et al.* Wound healing potential of curcumin cross-linked chitosan/polyvinyl alcohol. *Int J Biol Macromol* 2019; 140: 871-876.
8. Zhang X, Huo D, Wei J, Wang J, Zhang Q, Yang Q, *et al.* Synthesis of amino-functionalized nanocellulose by guanidine based deep eutectic solvent and its application in fine fibers retention. *Int J Biol Macromol* 2024; 260: 129473.
9. Wang F, Zhang W, Li H, Chen X, Feng S, Mei Z. How Effective are Nano-Based Dressings in Diabetic Wound Healing? A Comprehensive Review of Literature. *Int J Nanomedicine* 2022; 17: 2097-2119.
10. Yu H, Chen D, Lu W, *et al.* Characterization of polyvinyl alcohol/chitosan nanofibers loaded with royal jelly by blending electrospinning for potential wound dressings. *Int J Biol Macromol* 2025; 307: 141977.

Design and optimization of chitosan-based nanofibrous scaffold for the delivery of natural bioactive compounds

11. Wang Z, Zhao F, Xu C, *et al.* Metabolic reprogramming in skin wound healing. *Burns Trauma* 2024; 12: tkad047.
12. Ali A, Shahid MdA, Hossain MdD, Islam MdN. Antibacterial bi-layered polyvinyl alcohol (PVA)-chitosan blend nanofibrous mat loaded with *Azadirachta indica* (neem) extract. *Int J Biol Macromol* 2019; 138: 13-20.
13. Islam MdS, Rahaman MdS, Yeum JH. Electrospun novel super-absorbent based on polysaccharide-polyvinyl alcohol-montmorillonite clay nanocomposites. *Carbohydr Polym* 2015; 115: 69-77.
14. Păduraru L. RP-HPLC method with UV detection for the evaluation of chitosan-graft- β -cyclodextrin/PVA hydrogels as carriers for the controlled release of vemurafenib. *Med-Surg J - Rev Med Chir Soc Med Nat Iasi* 2025; 129(2): 459-479.
15. Nathan KG, Genasan K, Kamarul T. Polyvinyl Alcohol-Chitosan Scaffold for Tissue Engineering and Regenerative Medicine Application: A Review. *Mar Drugs* 2023; 21(5): 304.
16. Nitti P, Gallo N, Palazzo B, *et al.* Effect of L-Arginine treatment on the *in vitro* stability of electrospun aligned chitosan nanofiber mats. *Polym Test* 2020; 91:106758.
17. Eslami-Farsani M, Moslehi A, Hatami-Shahmir A. Allantoin improves histopathological evaluations in a rat model of gastritis. *Physiol Int* 2018; 105(4): 325-334.
18. Fernandes J, de Amorim GC, da Veiga TE, *et al.* Allantoin reduces cell death induced by cisplatin: possible implications for tumor lysis syndrome management. *JBIC* 2019; 24(4): 547-562.
19. Marchetti M, Ronda L, Percudani R, Bettati S. Immobilization of Allantoinase for the Development of an Optical Biosensor of Oxidative Stress States. *Sensors* 2019; 20(1): 196.
20. Selamoglu Z, Dusgun C, Akgul H, Fuat Gulhan M. *In-vitro* Antioxidant Activities of the Ethanolic Extracts of Some Contained-Allantoin Plants. *Shaheed Beheshti University of Medical Sciences and Health Services Iranian Journal of Pharmaceutical Research*. 2017.
21. Sakthiguru N, Sithique MA. Fabrication of bioinspired chitosan/gelatin/allantoin bio composite film for wound dressing application. *Int J Biol Macromol* 2020; 152: 873-883.
22. Conti V, Corbi G, Iannaccone T, *et al.* Effectiveness and Tolerability of a Patch Containing Onion Extract and Allantoin for Cesarean Section Scars. *Front Pharmacol* 2020; 11.
23. Nelson KM, Dahlin JL, Bisson J, Graham J, Pauli GF, Walters MA. The Essential Medicinal Chemistry of Curcumin. *J Med Chem* 2017; 60(5): 1620-1637.
24. Celebioglu A, Uyar T. Fast-dissolving antioxidant curcumin/cyclodextrin inclusion complex electrospun nanofibrous webs. *Food Chem* 2020; 317: 126397.
25. Lupascu F. Design and optimization method for obtaining pioglitazone and curcumin-loaded chitosan nanoparticles. *Med-Surg J - Rev Med Chir Soc Med Nat Iasi* 2022; 126(1): 126-134.
26. Bigham-Sadegh A, Torkestani HS, Sharifi S, Shirian S. Effects of concurrent use of royal jelly with hydroxyapatite on bone healing in rabbit model: radiological and histopathological evaluation. *Heliyon* 2020; 6(7): e04547.
27. Ahmad S, Campos MG, Fratini F, Altaye SZ, Li J. New Insights into the Biological and Pharmaceutical Properties of Royal Jelly. *Int J Mol Sci* 2020; 21(2): 382.
28. Lin Y, Zhang M, Wang L, *et al.* The *in vitro* and *in vivo* wound-healing effects of royal jelly derived from *Apis mellifera L.* during blossom seasons of *Castanea mollissima Bl.* and *Brassica napus L.* in South China exhibited distinct patterns. *BMC* 2020; 20(1): 357.
29. Lin Y, Zhang M, Lin T, *et al.* Royal jelly from different floral sources possesses distinct wound-healing mechanisms and ingredient profiles. *Food Funct* 2021; 12(23): 12059-12076.
30. Olczyk P, Koprowski R, Kaźmierczak J, *et al.* Bee Pollen as a Promising Agent in the Burn Wounds Treatment. *Evid Based Complement Alternat Med* 2016; 2016(1): 292379.
31. Ionescu OM. Design and optimization method for obtaining new chitosan-based nanofibers for wound healing applications. *Med-Surg J - Rev Med Chir Soc Med Nat Iasi* 2022; 126(1): 118-125.